Intersonic Crack Propagation along Interfaces: Experimental Observations and Analysis

by M. Kavaturu, A. Shukla and A. J. Rosakis

ABSTRACT—The isochromatic fringe patterns surrounding an intersonically propagating interface crack are developed and characterized using the recently developed stress field equations. A parametric investigation is conducted to study the influence of various parameters such as the crack-tip velocity and the contact coefficient on the isochromatic fringe patterns. It has been observed that the crack-tip velocity has a significant effect on the size and shape of isochromatic fringe patterns. The contact coefficient, on the other hand, does not affect the fringe pattern significantly. The paper also presents a numerical scheme to extract various parameters of interest such as the series coefficients of the stress field, the contact coefficient and the dissipation energy. The results show that the crack growth is highly unstable in the intersonic regime, and the energy dissipation decreases monotonically with increasing crack-tip velocity. The experimental data fit well with the recently proposed fracture criterion for intersonic interfacial fracture.

Introduction

Research in the area of dynamic interfacial fracture mechanics has been focused primarily on the study of the subsonic regime (crack-tip velocities lower than the lower of the two Rayleigh wave speeds in the bimaterial system) of dynamic crack growth. The first experimental evidence of high-speed subsonic crack growth in bimaterial interfaces was presented by Tippur and Rosakis.[1] This work demonstrated that crack-tip speeds in these systems may easily approach the lower of the two Rayleigh wave speeds of the bimaterial, suggesting the possibility of intersonic crack growth. Motivated by these early observations, a number of theoretical and numerical investigations have been carried out to address some of the fundamental issues related to the fracture of bimaterial interfaces in the subsonic regime.[2-5]

The steady-state asymptotic nature of the near-tip field of a crack propagating along an interface was provided by Yang et al.[2] For the more general transient crack growth case, higher order asymptotic stress field equations for subsonic fracture at nonuniform speeds along interfaces were provided by Liu et al.[6] These near-tip analytical developments provided the means of interpreting the experimental measurements and extracting the fracture parameters necessary for quantitative analysis of the phenomenon. Equipped

with these analyses, Lambros and Rosakis[7] used CGS interferometry to study interfacial crack growth in the subsonic regime and subsequently proposed the first fracture criterion describing dynamic interfacial crack growth. Subsequently, Singh et al.[8] developed a special specimen geometry to study the initiation, propagation and arrest of an interface crack subjected to an explosively generated planar tensile wave. Finally, Kavaturu and Shukla[9] proposed an improved criterion that establishes a generalized relationship between the dynamic energy release rate and the instantaneous crack-tip velocity.

The work of Yang et al.[2] was the first analytical investigation to suggest the theoretical possibility of intersonic crack growth in bimaterials. They demonstrated that as the crack-tip speed approaches the lower Rayleigh wave speed, the dynamic energy release rate remains finite. Indeed, recent experimental studies[10-12] in the area of intersonic fracture of bimaterial interface have revealed some interesting physical phenomena. Using the optical method of CGS and high-speed photography, Lambros and Rosakis[10] observed that under shear-dominated loading conditions, the interfacial crack tip can exceed both the Rayleigh and shear wave velocities of the more compliant half in the bimaterial. They also reported visual experimental evidence of large-scale crack face contact occurring during intersonic crack growth. In a companion paper, Liu et al.[13] obtained the two-dimensional in-plane, asymptotic deformation fields surrounding a traction-free crack tip propagating intersonically along an elastic-rigid bimaterial interface. Results of this analysis showed that the near-tip stress fields do not exhibit oscillations as in the case of subsonic fracture and that the stress singularity at the crack tip is a function of the crack-tip speed. This analysis also predicted the existence of a mach wave that radiates from the crack tip and moves with it. Across this mach wave, the particle velocities and the stresses suffer infinite jumps. In the velocity range, $c_s < v < \sqrt{2C_s}$, the theoretical analysis predicted either crack-face interpenetration or negative normal traction ahead of the crack tip. This observation was consistent with the visual evidence of large-scale crack-tip contact reported by Lambros and Rosakis.[10] The prediction of a mach wave radiating from the crack tip was, however, conclusively verified only later by Singh and Shukla[11] and Singh et al.[12] by means of photoelasticity and high-speed photography. These investigators also corroborated the existence of a large-scale contact of crack faces behind the interfacial crack tip. In their work, a secondary mach wave emanating from the trailing edge of the contact zone was also observed in addition to the primary mach wave (i.e., the mach wave associated with the crack tip).

M. Kavaturu (SEM Member) is a Senior Research Engineer, Goodyear Tire & Rubber Company, Akron, OH, and A. Shukla (SEM Fellow) is Professor, Dynamic Photomechanics Laboratory, Department of Mechanical Engineering and Applied Mechanics, University of Rhode Island, Kingston, RI 02881. A. J. Rosakis (SEM Executive Board Member) is Professor, Graduate Aeronautical Laboratories, California Institute of Technology, Pasadena, CA 91125.

Very recently, Huang et al.[14] reanalyzed steady-state interfacial crack growth allowing for crack face contact. Their results clearly predict most of the essential qualitative features of experimental observations discussed earlier in this section. The method of analytical continuation was used to obtain the in-plane deformation and stress fields. This work provided a means for analyzing the experimentally obtained CGS and photoelastic fringe patterns in the intersonic regime.

In the present work, the stress field equations developed by Huang et al.[14] were used to develop and characterize the isochromatic fringe patterns in the intersonic regime. Furthermore, the dependence of the fringe patterns on various fracture parameters such as the contact coefficient and the crack-tip velocity has been investigated. The paper also presents a numerical scheme to extract various parameters of interest such as the coefficients of the stress series, the contact coefficient and the dissipation energy. A nonlinear least squares method based on the Levenberg-Marquardt scheme[15] was used to analyze the isochromatic fringe patterns obtained from experiments involving the fracture of Homalite-100/aluminum bimaterial specimens. The specimens were subjected to impact by a projectile fired from a gas gun which results in crack initiation and subsequent propagation. The entire fracture event was photographed using dynamic photoelasticity in combination with high-speed photography. The experimental results validated the fracture criterion proposed by Huang et al.[14]

Theoretical Considerations

Crack-tip Stress Field Equations

Consider a crack propagating intersonically along an elastic-rigid bimaterial interface as shown in Fig. 1. The velocity of crack propagation v is assumed to be more than the shear wave speed of the elastic half of the bimaterial system. As shown in the figure, the contact zone has a length l at the elastic-rigid interface. A linear model[14] is used to relate the shear and normal stresses within the contact zone, and a traction-free boundary condition was used for crack face outside the contact zone as

$$\begin{array}{lll} \sigma_{12} = \lambda\sigma_{22} & u_2 = 0 & -l < \eta_1 < 0 \\ \sigma_{12} = 0 & \sigma_{22} = 0 & \eta_1 < -l, \end{array} \tag{1}$$

where λ is the contact coefficient which is analogous to the classical friction coefficient. The stress field in the elastic solid above the interface can be expressed as

$$\sigma_{11} = \mu\left[(1 + 2\alpha_1^2 + \hat{\alpha}_s^2)\mathrm{Re}\{F''(z_l)\} + 2\hat{\alpha}_s g''(\eta_1 + \hat{\alpha}_s\eta_2)\right]$$

$$\sigma_{22} = \mu\left[(1 - \hat{\alpha}_s^2)\mathrm{Re}\{F''(z_l)\} + 2\hat{\alpha}_s g''(\eta_1 + \hat{\alpha}_s\eta_2)\right]$$

$$\sigma_{12} = \mu\left[2\alpha_l\mathrm{Im}\{F''(z_l)\} + (1 - \hat{\alpha}_s^2)g''(\eta_1 + \hat{\alpha}_s\eta_2)\right], \tag{2}$$

where F is an analytical function of z_l in the upper half plane, $\eta_2 \geq 0$, g is a real function of its argument, μ is the shear modulus of the elastic material and

$$\alpha_l = \left(1 - \frac{v^2}{c_l^2}\right)^{1/2} \qquad \hat{\alpha}_s = \left(\frac{v^2}{c_s^2} - 1\right)^{1/2}, \tag{3}$$
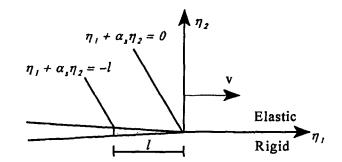

Fig. 1—Schematic of the interface crack propagating intersonically along an elastic-rigid bimaterial interface

where v is the crack-tip velocity and c_s and c_l are the shear and longitudinal velocities of the elastic material, respectively.

Substitution of stresses [eq (2)] into boundary conditions [eq (1)] results in a Riemann-Hilbert problem. Solution to this problem results in the stress field as

$$\sigma_{ij} = \mu \sum_{n=0}^{\infty} B_n s_{ij}(\eta_1, \eta_2, q - n, p), \tag{4}$$

where q and p are the strength of singularity at the crack tip and at the trailing end of the contact zone, respectively. These singularities q and p are observed to be dependent on the crack-tip velocity. s_{ij}, which are functions of q, p and positional coordinates (η_1, η_2), are defined in Huang et al.[14]

The energy dissipated in the contact zone over unit contact length D using the dominant leading term of the stress series expansion is given by

$$D = \frac{\mu B_0^2}{l^{2(q+p)-1}}G(v, \lambda), \tag{5}$$

where B_0 is the leading coefficient of the stress series and G is a function of the crack-tip velocity and the contact coefficient.[14]

Characterization of Isochromatic Fringe Patterns

The isochromatic fringe patterns in a photoelastic material represent the contours of constant maximum shear stress which are governed by the stress-optic law given by

$$\frac{Nf_\sigma}{2h} = \frac{\sigma_1 - \sigma_2}{2} = \sqrt{\left(\frac{\sigma_{11} - \sigma_{22}}{2}\right)^2 + \sigma_{12}^2}, \tag{6}$$

where N is the fringe order, f_σ is the material fringe constant and h is the thickness of the material. Substitution of eq (4) in (6) results in an equation which was used to generate the isochromatic fringe patterns surrounding the crack tip for a given elastic material, leading term in the stress series expansion B_0, crack-tip velocity v, contact length l and contact coefficient λ. Contours of the fringe order N represent the isochromatic fringe patterns in the elastic half of the bimaterial. It should be mentioned here that only the leading term of the stress series was considered to develop the isochromatic fringe patterns. The elastic material chosen in this study was Homalite-100, a birefringent polyester supplied by Homalite Corporation. The material properties of Homalite-100 are listed in Table 1.

TABLE 1—MATERIAL PROPERTIES OF HOMALITE-100 AND ALUMINUM

Property	Homalite-100	6061 Al
Young's modulus, E(GPa)	5.3	71
Poisson's ratio, v	0.35	0.33
Density, ρ (kg/m^3)	1230	2770
P-wave velocity, c_1 (m/s)	2220	5430
S-wave velocity, c_s (m/s)	1270	3100
Rayleigh velocity, c_R (m/s)	1186	2890
Fracture toughness, K_{ic} (MPa$\sqrt{m}$)	0.45	29
Material fringe value, f_σ (kN/m)	23.7	
Mismatch parameter, ϵ		0.0912

Sensitivity of Isochromatics to Various Fracture Parameters

EFFECT OF CRACK-TIP VELOCITY

In order to study the effect of crack-tip velocity, a set of isochromatic fringe patterns were generated keeping λ, l and B_0 constant and varying the crack-tip velocity. Isochromatic fringe patterns surrounding the crack tip as a function of crack-tip velocity are shown in Fig. 2. As can be seen from the figure, a direct consequence of the variation of crack-tip velocity is its effect on the inclination of the line discontinuities or mach waves (primary and secondary). As the crack-tip velocity increases, the inclination of the mach waves (measured counterclockwise from positive η_1-axis) increases. This fact was experimentally corroborated by Singh and Shukla.[11] Also, it is clearly evident that the singularity at the crack tip is stronger than that at the end of the contact zone. Indeed, experimental observations by Singh and Shukla[11] and Singh et al.[12] confirm that the mach wave originating from the crack tip is stronger than that emanating from the end of contact zone. Fig. 2 also shows that, as the crack-tip velocity increases, the fringes close to the crack tip and the fringes inside the contact zone increase in number and size, clearly indicating that the isochromatics are sensitive to changes in the crack-tip velocity.

EFFECT OF THE LEADING TERM B_0 OF THE STRESS SERIES

The leading term B_0 of the stress series is analogous to the classical stress intensity factor and completely characterizes the near-tip stress fields in the intersonic regime. Simple intuition suggests that this term either magnifies or shrinks the isochromatic fringe patterns surrounding the crack tip. However, in order to verify if this parameter could be extracted from the isochromatic fringe patterns, the sensitivity of the fringe patterns to the change in the value of B_0 needs to be investigated. The sensitivity is defined as the rate of change of the fringe order per unit change in $B_0(dN/dB_0)$. The sensitivity at a point (5 mm, 5 mm) was calculated to be approximately 4000, i.e., a change of 0.001 in B_0 gives rise to a change of 4 fringe orders. Thus, it can be concluded that the isochromatics are extremely sensitive to the value of B_0.

EFFECT OF CONTACT COEFFICIENT

Figure 3 shows the effect of the contact coefficient on the isochromatic fringe patterns for crack propagation along Homalite-100/rigid bimaterial. In this figure, isochromatics are generated for $\lambda = 0.1$, 1 and 10. It should be mentioned here that although the contact coefficient is similar to the clas-

sical friction coefficient, it can be greater than one because the cracked interface may be rough and serrated, which may cause locking at the interface to provide resistance against sliding.[14] The variation of fringe order at a point (-5 mm, 5 mm) inside the contact zone is plotted as a function of the contact coefficient in Fig. 4. Although the isochromatic fringe patterns are sensitive to changes in the contact coefficient up to a value of 10, the fringe order is a relatively weak function of the contact coefficient $\lambda > 10$.

Extraction of the Fracture Parameters

It was demonstrated in the previous section that the isochromatic fringe patterns in the vicinity of the interfacial crack tip are sensitive to changes in various fracture parameters including the contact coefficient, the leading term of the stress series and the crack-tip velocity. Thus, all these parameters could be extracted from the isochromatics obtained from experiments by solving the inverse problem using an overdeterministic least squares method. A nonlinear least squares method based on the Levenberg-Marquardt scheme is adopted for the purpose of analysis. Using eqs (6) and (4), define the error of the kth point collected from a given isochromatic fringe pattern as

$$g_k(\lambda, B_0, B_1, B_2, \dots) = \left(\frac{N_k f_\sigma}{2h}\right)$$
$$- \sqrt{\left(\frac{\sigma_{11} - \sigma_{22}}{2}\right)^2 + \sigma_{12}^2}. \quad (7)$$

Now the iterative nonlinear least squares method attempts to find the minimum value of the function

$$F = \sum_{k=0}^{n} g_k^2, \quad (8)$$

where n is the total number of points collected from the fringe patterns. For a detailed discussion on implementation and theory of the Levenberg-Marquardt method, the reader may refer to Moré.[15]

To verify the method, the code was used to extract fracture parameters from a set of isochromatic fringe patterns generated with known values of $\lambda = \lambda^0 = 0.1$ and $B_0 = B^0 = 0.002$. The values obtained from the analysis ($\lambda^I = 0.094$ and $B_0^I = 0.0019$) matched λ^0 and B^0, thus validating the analysis procedure (Fig. 5). In fig. 5, symbols correspond to the digitized data from the numerically generated fringe pattern using the values λ^0 and B^0 and the solid lines represent the numerically generated fringe pattern with λ^I and

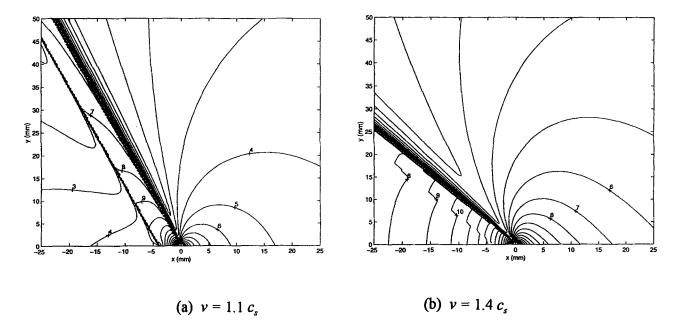(a) $v = 1.1\, c_s$ (b) $v = 1.4\, c_s$

Fig. 2—Isochromatic fringe pattern for intersonic crack propagation along Homalite-100/aluminum bimaterial interface as a function of crack-tip velocity
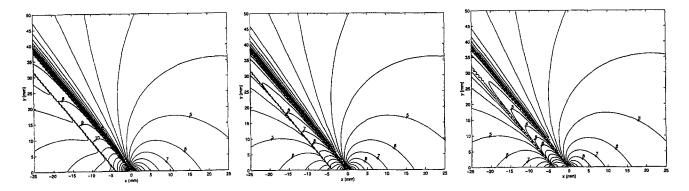

Fig. 3—Isochromatic fringe pattern for intersonic crack propagation along Homalite-100/aluminum bimaterial interface as a function of the contact coefficient
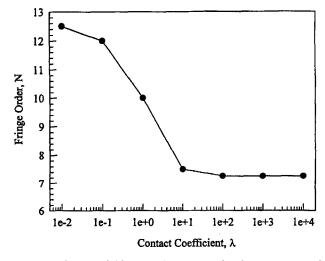

Fig. 4—Variation of fringe order at a point (-5 mm, 5 mm) inside the contact zone as a function of the contact coefficient

B_0^I. The error in the values obtained from the analysis is primarily due to the errors introduced during digitization of the isochromatics.

The analysis procedure established here was used to investigate the intersonic fracture of Homalite-100/aluminum bimaterial interface subjected to impact loading.

Experimental Procedures

Specimen Preparation

The bimaterial specimens used in this study were made of a stiff aluminum half bonded to a compliant Homalite-100 half (a birefringent polymer supplied by the Homalite Corporation). The mechanical properties of the bimaterial constituents are shown in Table 1. This bimaterial combination provides a significant (elastic) mismatch of properties across the interface to produce intensified interfacial effects at the crack tip. A sharp starter crack of 25 mm in length was in-
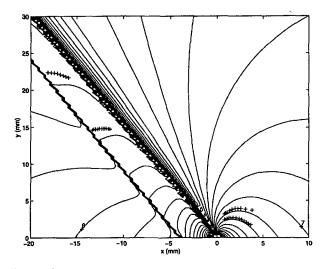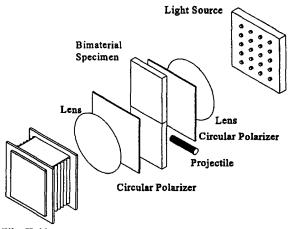
Fig. 5—Comparison of the digitized data points from the numerically generated fringes using $\lambda = 0.1$ and $B_0 = 0.002$ with the fit generated from the digitized data

Fig. 6—Experimental setup for investigating the fracture of a bimaterial interface subjected to impact loading

troduced at the bimaterial interface by means of Teflon® tape during the bonding process. The procedure for the specimen preparation is described in detail in Singh et al.[8]

Impact Loading Experiments

The schematic of the experimental setup used to investigate the fracture process is shown in Fig. 6. The bimaterial specimen was placed on the optical bench of the Cranz-Schardin high-speed camera. Schematic of the bimaterial specimen used to study the interfacial fracture under impact loading is shown in Fig. 7. The aluminum half of the bimaterial specimen was subjected to impact by a projectile fired from a gas gun at speeds on the order of 20 m/s. A steel projectile (13 mm diameter × 100 mm long) was used to impact the bimaterial specimens. The impact sets up a compressive wave in aluminum half which traverses the width of the specimen and reflects off the free surface as a tensile wave. This tensile wave loads the interface crack primarily in shear, resulting in crack initiation and subsequent propagation. The entire event of crack initiation and propagation was observed using dynamic photoelasticity in conjunction with high-speed photography. The high-speed camera provides a total of 20 photographs at framing rates on the order of a million frames per second. A sequence of photographs obtained in a typical impact loading experiment is shown in Fig. 8. Time $t = 0$ corresponds to the time of impact. These fringe patterns were recorded in the Homalite-100 half of the bimaterial specimen.

An enlarged photograph of the interface crack propagating in the intersonic regime is shown in Fig. 9. The line of discontinuity (primary mach wave) emanating from the crack tip and the large-scale contact of crack faces were observed. In the figure, the contact zone is characterized by fringes that run parallel to the interface. The secondary mach wave emanating from the end of contact zone was also observed in addition to the primary mach wave. It is clear from the figure that the density of fringes in the primary mach is less than that of the secondary mach. This implies that the secondary mach is weaker than the primary mach. The isochromatic fringe patterns also show another disturbance that trails the interson-
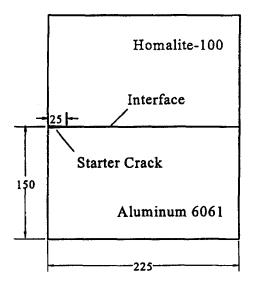

Fig. 7—Schematic of the specimen geometry used in the study

ically propagating interfacial crack tip. This was identified as a Rayleigh wave singularity that was generated when the crack tip accelerated through the Rayleigh wave velocity of Homalite-100.[16]

Results and Discussion

The velocity of the interfacial crack tip was calculated from the knowledge of the crack-tip location history obtained from the photographs. The history of the crack-tip velocity for a typical impact loading experiment is shown in Fig. 10. As can be seen from the figure, the crack tip quickly accelerated to shear wave velocity of Homalite-100 soon after crack initiation. Thereafter, the crack tip continued to increase at a smaller rate to around 140 percent of the shear wave speed of Homalite-100. The figure also shows the history of velocities of the end of the contact zone and the Rayleigh singularity. It can be seen from the figure that the Rayleigh singularity was traveling at the Rayleigh wave speed of Homalite-100. Also,
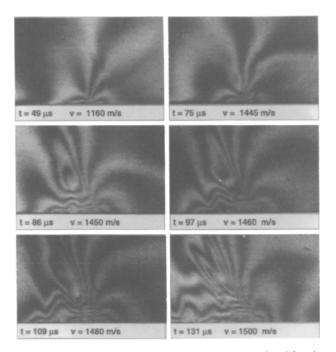
Fig. 8—Typical isochromatic fringe patterns obtained for dynamic fracture along Homalite-100/aluminum interface subjected to impact loading
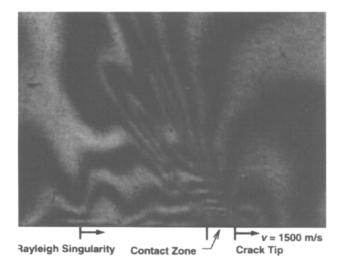

Fig. 9—Magnified photograph showing the isochromatics around the interfacial crack tip in the intersonic regime. Photograph also shows the primary and the secondary shock fronts, the contact zone and the Rayleigh wave singularity

the trailing end of the contact zone had the same velocity as the interfacial crack tip.

The isochromatic fringe patterns surrounding the crack tip were analyzed using higher order stress field equations detailed in previous sections. A total of 40 data points was collected from the fringes ahead of the crack tip and the fringes inside the contact zone. A typical result of the least squares fit is shown in Fig. 11. In the figure, the solid lines are contours of maximum shear stress obtained numerically by using the results of higher order least squares fit generated by the sampled data, and the symbols correspond to the data points sampled from the experimental photographs. It is clear from the figure that the experimental data fit well qualitatively with
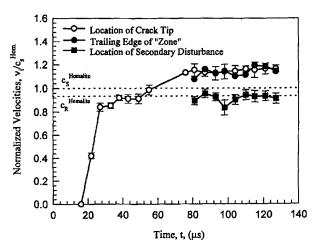

Fig. 10—Histories of velocity of the crack tip, the trailing end of the contact zone and the Rayleigh wave singularity
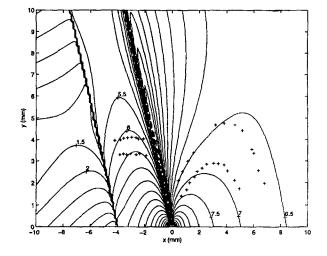

Fig. 11—Comparison of the digitized data points from the isochromatics obtained from a typical experiment with the fit generated from the digitized data

the fringes generated by the least squares fit. However, the data did not fit satisfactorily with the fringes inside the contact zone. This is primarily because the synthetic fringe pattern is characterized by curved sets of fringes inside the contact zone. In contrast, the photographs obtained from the experiment have fringes that are flat and parallel to the interface. This may be an artifact of the assumption of velocity independent contact coefficient. Nonetheless, the fringe orders of the data points collected from the photographs were observed to match those of the numerically developed fringe pattern.

Critical Crack Face Sliding Displacement Failure Criterion

Huang et al.[14] have proposed a criterion for intersonic crack growth along bimaterial interfaces. This criterion is based on the premise that the crack growth occurs in the presence of constant critical sliding displacements (δ_c) evaluated at the end of the contact zone, i.e.,

$$u_1(\eta_1, = -l, \eta_2 = 0^+) = \delta_c. \tag{9}$$

This was primarily motivated by the criterion proposed for subsonic interfacial crack growth by Lambros and Rosakis.[7]

This criterion establishes a relationship between the leading term of the stress series B_0 and the crack-tip velocity v given by

$$B_0 = \frac{\delta_c l^{p+q-1}}{\beta(1-q, 1-p)\sin(q\pi)}, \tag{10}$$

where $\beta(x, y)$ is the β-function defined by

$$\beta(x, y) = \int_0^1 t^{x-1}(1-t)^{y-1}. \tag{11}$$

Equation (10) can be used to obtain a functional relationship between the dissipation energy and the crack-tip velocity given by

$$\frac{D}{\mu\delta_c^2/l} = \frac{\beta(1-2q, 1-2p)}{\sin^2(q\pi)[\beta(1-q, 1-p)]^2}$$

$$\cdot \frac{\lambda\alpha_l^2\left(1+\hat{\alpha}_s^2\right)^2\left(1-\hat{\alpha}_s^2\right)(1+\lambda\hat{\alpha}_s)}{\left[\alpha_l^2\hat{\alpha}_s\left(1+\hat{\alpha}_s^2\right)^2+\lambda\left(1-\hat{\alpha}_s^2+2\alpha_l^2\hat{\alpha}_s\right)\right]^2}$$

$$\frac{1}{+\left[\alpha_l\left(1+\hat{\alpha}_s^2\right)^2(1+\lambda\hat{\alpha}_s)\right]^2}. \tag{12}$$

Equations (10) and (12) are plotted along with the experimental data in Figs. 12(a) and 12(b), respectively, for different values of λ: 0.1, 1 and 10. The values of λ are so chosen because the values of λ obtained from the experiments fall within this range. The lines in Fig. 12 represent the criterion, and the symbols denote the experimental data. The critical sliding displacement δ_c was eliminated from equation (10) by normalizing with the corresponding value at $v = 1.05c_s$.

It is clear from the figure that the data show a reasonable agreement with the critical sliding displacement criterion. Additionally, B_0 and D reduce monotonically with the crack-tip velocity. This decreasing trend in the dissipation energy is characteristic of unstable crack propagation $(dD/dv < 0)$. The theoretical analysis by Liu et al.[13] predicts that, in the velocity range $c_s < v < \sqrt{2C_s}$ either crack face contact or negative traction ahead of the crack tip occurs, suggesting that this velocity regime is unfavorable for stable crack growth. The data plotted in Fig. 12 fall in the above velocity range, thus reconfirming the observations made in this theoretical analysis.

Very similar results were observed by Andrews,[17] who performed numerical calculations on cracks propagating in homogeneous materials under predominant shear conditions. He deduced that under shear-dominated conditions, stable crack propagation could only occur in the velocity regimes $0 < v < c_R$ and $\sqrt{2C_s} < v < c_l$ (longitudinal wave velocity).

Conclusions

The isochromatic fringe patterns surrounding the crack tip were developed and characterized using the recently developed stress field equations. The dependence of isochromatic fringe patterns on various fracture parameters such as the
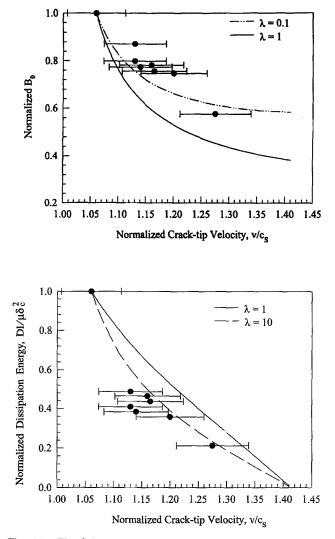

Fig. 12—Fit of the experimental data with the critical crack face sliding criterion

contact coefficient and the crack-tip velocity has been investigated. It was found that the crack-tip velocity has a significant effect on the size, shape and number of fringes surrounding the crack tip. The contact coefficient, on the other hand, was found not to have a considerable effect on the isochromatic fringe patterns. The paper also presents a numerical scheme to extract various parameters of interest such as the coefficients of the stress series, the contact coefficient and the dissipation energy. A nonlinear least squares method based on the Levenberg-Marquardt scheme was used to analyze the isochromatic fringe patterns obtained from experiments involving the fracture of a Homalite-100/aluminum bimaterial specimen. The results show that the crack growth is highly unstable in the intersonic regime. The experimental data were also used to validate a recently proposed criterion for intersonic crack growth along bimaterial interfaces.

References

1. Tippur, H.V. and Rosakis, A.J., "Quasi-static and Dynamic Crack Growth Along Bimaterial Interfaces: A Note on Crack-tip Field Measurements Using Coherent Gradient Sensing," EXPERIMENTAL MECHANICS, 31, 243–251 (1991).

2. Yang, W., Suo, Z., and Shih, C.H., "Mechanics of Dynamic Debonding," Proc. Roy. Soc. Lon., A433, 679–697 (1991).

3. Deng, X., "Complete Complex Series Expansions of Near-tip Fields for Steadily Growing Interface Cracks in Dissimilar Isotropic Materials," Eng. Fract. Mech. 42, 237–242 (1992).

4. Nakamura, T., "Three Dimensional Stress Fields of Elastic Interface Cracks," J. App. Mech. 58, 939–946 (1991).

5. Xu, X.-P. and Needleman, A., "Numerical Simulations of Dynamic Crack Growth Along an Interface," Int. J. Fract., 74, 289–324 (1996).

6. Liu, C., Lambros, J., and Rosakis, A.J., "Highly Transient Elastodynamic Crack Growth in a Bimaterial Interface: Higher Order Asymptotic Analysis and Optical Experiments," J. Mech. Phys. Solids, 41, 12, 1857–1954 (1993).

7. Lambros, J., and Rosakis, A.J., "Development of a Dynamic Decohesion Criterion for Subsonic Fracture of the Interface Between Two Dissimilar Materials," Proc. Roy. Soc. Lon. A451, 711–736 (1995).

8. Singh, R.P., Kavaturu, M., and Shukla, A., "Initiation, Propagation and Arrest of a Bimaterial Interface Crack Subjected to Controlled Stress Wave Loading," Int. J. Fract., 83, 291–304 (1997).

9. Kavaturu, M. and Shukla, A., "Dynamic Fracture Criteria for Crack Growth Along Bimaterial Interfaces," J. Appl. Mech., 65, 293–299 (1998).

10. Lambros, J. and Rosakis, A.J., "Shear Dominated Transonic Crack Growth in Bimaterials, Part I: Experimental Observations," J. Mech. Phys. Solids, 43, 169–188 (1995).

11. Singh, R.P. and Shukla, A., "Subsonic and Transonic Crack Growth Along a Bimaterial Interface," J. Appl. Mech. 63, 919–924 (1996).

12. Singh, R.P., Lambros, J., Shukla, A., and Rosakis, A.J., "Investigation of the Mechanics of Intersonic Crack Propagation Along a Bimaterial Interface Using Coherent Gradient Sensing and Photoelasticity," Proc. Roy. Soc. Lon., 453, 2649–2667 (1997).

13. Liu, C., Huang, Y., and Rosakis, A.J., "Shear Dominated Transonic Interfacial Crack Growth in a Bimaterial-II. Asymptotic Fields and Favorable Velocity Regimes," J. Mech. Phys. Solids, 43, 189–206 (1995).

14. Huang, Y., Wang, W., Liu, C., and Rosakis, A.J., "Intersonic Interfacial Crack Growth in a Bimaterial: An Investigation of Crack Face Contact," manuscript submitted (1997).

15. Moré, J.J., "The Levenberg-Marquardt Algorithm: Implementation and Analysis," Numerical Analysis, ed. G.A. Watson, Lecture Notes in Mathematics 630, Springer Verlag, 105–116 (1977).

16. Freund, L.B., "Response of an Elastic Solid to Nonuniformly Moving Surface Loads," J. Appl. Mech., 40, 699–704 (1979).

17. Andrews, D.J., "Rupture Velocity in Plane Strain Shear Cracks," J. Geophysical Res., 81, 5679–5687 (1976).